PREDICTABILITY AND BAROCLINIC FLOW REGIMES

B. Legras and R. Vautard
Laboratoire de Météorologie Dynamique
Paris, France

Introduction

In 1979, Charney and De Vore brought to light the possible existence of multiple regimes in the atmospheric flows, an idea already popular during the fifties (Baur, 1951) that was seemingly completely overlooked during the next decade. A main motivation was the observation of the index cycle in mid-latitudes and the alternation of zonal and blocking dominated circulation over the preferred areas of low frequency variability, i.e. the western margins of the continents and northern Siberia (Dole and Gordon, 1983).

Objective arguments in favor of multiple regimes from atmospheric observations lie in two classes :

1) The direct observation of bimodality in the wave activity (Sutera, Hansen, 1985) ;

2) The exponential decrease of the distribution of persistence durations (Dole and Gordon, 1983). Should the source of variability be purely linear, the distribution of persistence durations would exhibit a peak at a preferred time scale.

The consequence for predictability is that the weather regime does not follow linearly the variations of the external conditions - which can be partly imposed in mid-latitudes by propagation of tropical influences - but is largely governed by internal variability characterized by transition properties between different equilibria. The variations of external conditions are likely to modulate these properties. It must be added that complete triggering of the weather regime by external conditions is recovered if transition properties vary very rapidly with the external conditions (Egger, 1981; Benzi et al., 1984) or if multiple equilibria exist only in a narrow range of parameters. In this case, hysteresis effects (Kallen, 1985; Tung and Rosenthal, 1985) may induce alternation of persistence and rapid transitions.

One of the major drawbacks of the theory of multiple equilibria is the fact that the range of parameters and the mechanisms involved in the barotropic models in which they have been first investigated (Charney and De Vore, 1979 ; Charney et al., 1981 ; Källén,1984 ; Legras and Ghil, 1985) are not supported by observations (Tung and Rosenthal, 1985). Large wind forcing and small dissipation are required, which can only be justified on heuristic basis. In addition, the form-drag conversion in the energetics must be considerably larger than observed in order to maintain the waves and to induce transitions between regimes. Indeed there exists no clear way to simulate in a pure barotropic model the baroclinic conversion that dominates the generation of eddy kinetic energy in the atmosphere.

The need of form-drag conversion disappears in studies which follow a baroclinic approach. Charney and Strauss (1980) found that stationary baroclinic instability can be triggered by orography while involving essentially baroclinic conversion to maintain the waves. Reinhold and Pierrehumbert (1982) showed that a low order baroclinic model with orography exhibits different regimes in the sense that trajectories in phase space seem to be confined in at least two rather separated 'clouds' with transitions between them induced by synoptic scales. As noticed also by Itoh (1985), the averaged energetics of chaotic baroclinic dynamics differs significantly from the energetics of stationary states and of the most unstable modes.

Some recent observations of Atlantic blocking cases (Illari and Marshall, 1983) show that synoptic-scale activity contributes significantly to the onset and the maintenance of the block. This is also apparent from analyses of mean-flow forcing by the transients (Hoskins et al., 1983) and is consistent with numerical studies of the nonlinear development of baroclinic instability (Simmons and Hoskins, 1978).

The ability of diffluent jets to be reinforced by travelling disturbances was shown by Shutts (1983) in a pure barotropic framework. His result suggests a baroclinic mechanism of blocking generation, already mentioned by Hoskins et al. (1983), which does not involve any dynamical orographic effect. Namely, baroclinic disturbances generated in large shear areas on Eastern margins of the continents mature as they propagate downstream along storm tracks, turn to a barotropic profile, and transfer their energy to large-scale barotropic dipoles at the exit of the storm track.

Two-layer baroclinic model

In order to test this idea, we investigate a two-layer quasi-geostrophic model in a periodic channel in which a localized baroclinic jet is maintained. In standard notations, the equations read

upper layer

$$\frac{\partial}{\partial t} q_1 + J(\psi_1, q_1) + U_1 \frac{\partial q_1}{\partial x} + (\beta + R_1^{-2}(U_1 - U_2)) \frac{\partial \psi_1}{\partial x}$$

$$= \Theta_1 + R_1^{-2} \nu_i \Delta(\psi_2 - \psi_1) - (\alpha \frac{\partial^8}{\partial x^8} + \alpha' \frac{\partial^8}{\partial y^8}) q_1 - D_{pe} \qquad (1)$$

lower layer

$$\frac{\partial}{\partial t} q_2 + J(\psi_2, q_2) + U_2 \frac{\partial q_2}{\partial x} + (\beta + R_2^{-2}(U_2 - U_1)) \frac{\partial \psi_2}{\partial x}$$

$$= \Theta_2 + R_2^{-2} \nu_i \Delta(\psi_1 - \psi_2) - (\alpha \frac{\partial^8}{\partial x^8} + \alpha' \frac{\partial^8}{\partial y^8}) q_2 - \nu_e R_2^{-2} \Delta \psi_2 \qquad (2)$$

with $q_1 = \Delta\psi_1 + R_1^{-2}(\psi_2-\psi_1)$

$q_2 = \Delta\psi_2 + R_2^{-2}(\psi_1-\psi_2)$

The characteristic parameters are listed below

- channel width : 7000 km, length : 28 000 km, centered at 45°

- isentropic levels : lower 296K upper 323K

- resolution 21 × 13 in spectral domain

- deformation radius : R_2 = 476 km R_1 = 707 km

- Ekman damping : 2 days

- Newtonian cooling : 10 days

- superviscous damping : 3h at k = 21 in longitude and l = 13 in latitude

- planetary scale damping : 13 days for k = 0,1
  26 days for k = 2

- mean wind : lower layer U_2 = 9,5 ms^{-1}, upper layer U_1 = 14,5 ms^{-1}

- baroclinic jet with maximum shear u_1-u_2 = 15 ms^{-1} maintained over 1/4 of the channel in the upper layer.

These parameters are believed to fall within the range of realistic values. The mean wind is such that the external mode (k = 3, l = 2) is stationary. The mean shear induces baroclinic instability in the range $5 \leqslant k \leqslant 9$ for the zonal wave number with an e-folding time larger than 5 days. The Rossby radius of deformation R_1 and R_2 are derived from the US Standard Atmosphere. They are found to be different at the two considered levels. An important consequence of this choice is that the stationary external mode (3,2) is less damped than the associated propagating internal mode.

The D_{pe} term which acts in the upper level is a selective damping over the largest zonal scales. Although small, this damping was found necessary to avoid excessive accumulation of energy within these modes. It can hardly be justified rigorously but it might account for the lack of vertical propagation to the stratosphere and horizontal propagation to the tropics in our model which affects preferentially the largest zonal scales in the atmosphere.

The G_1 and G_2 terms maintain as a stationary solution a baroclinic jet located over the first quarter of the channel, cf Fig.1.

Averaged flow

Fig.2 shows the averaged streamfunction at the upper level with the uniform wind contribution removed. The dominating pattern is a jet in the middle of the channel which extends downstream of the forced circulation. The total variance of the streamfunction at mid-level, Fig. 3, concentrates along the jet and in two branches which split at the exit of the jet. The total eddy heat variance, Fig. 4, concentrates along the jet and the fluxes act mainly to destroy the imposed baroclinicity. The total eddy vorticity variance and fluxes, not shown, exhibit very similar pattern.

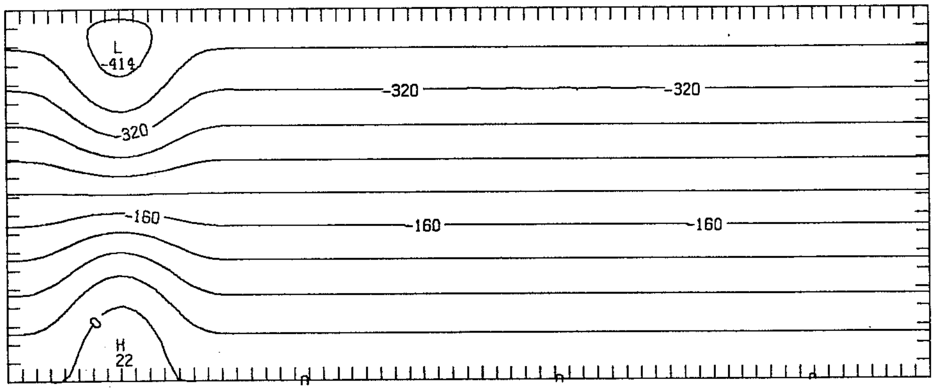

Figure 1 : Streamfunction of the imposed stationary solution in the upper layer.

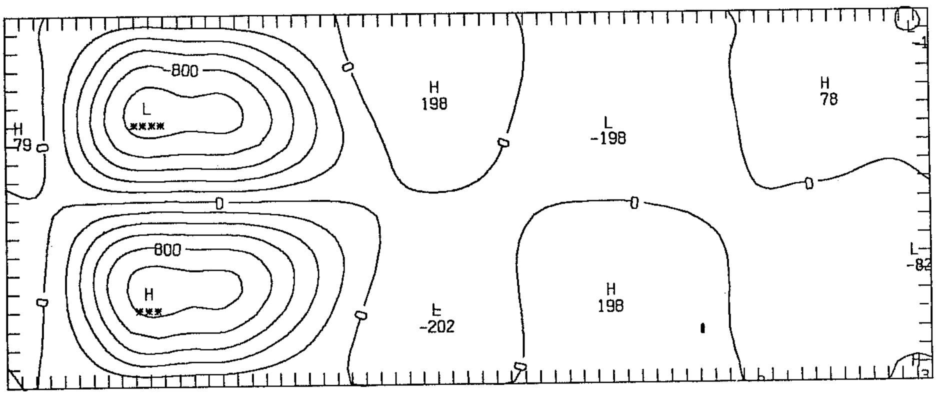

Figure 2 : Averaged streamfunction at the upper level with the uniform wind contribution removed.

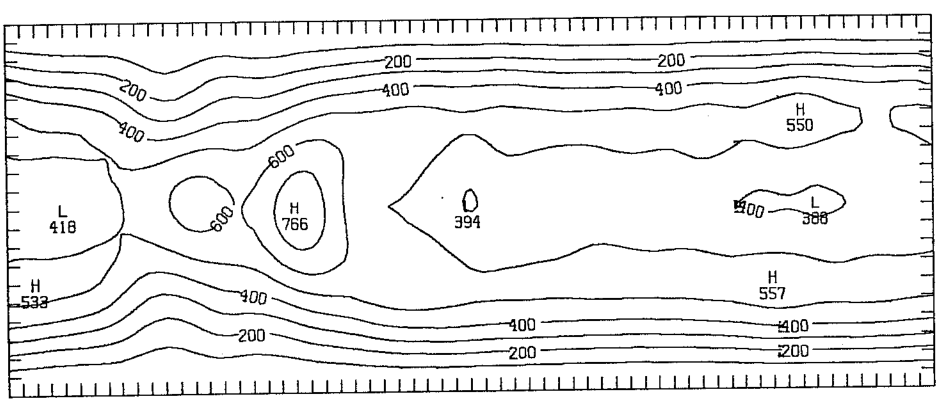

Figure 3 : Total variance of the streamfunction interpolated at mid-level.

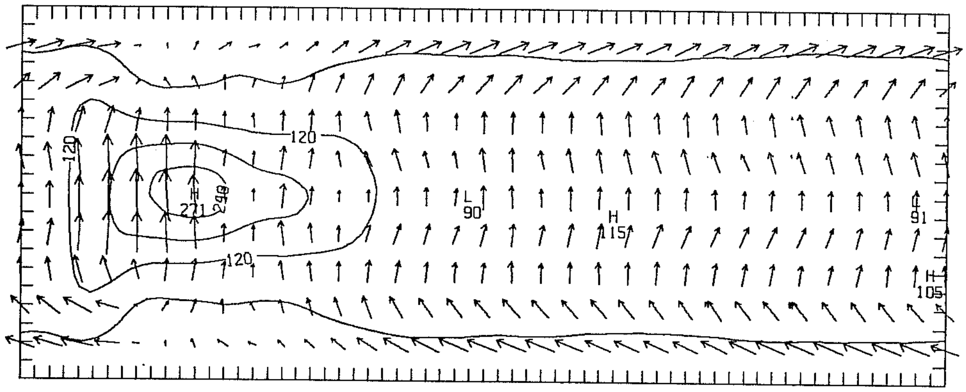

Figure 4 : Total eddy heat variance and fluxes (arrows) at mid-level.

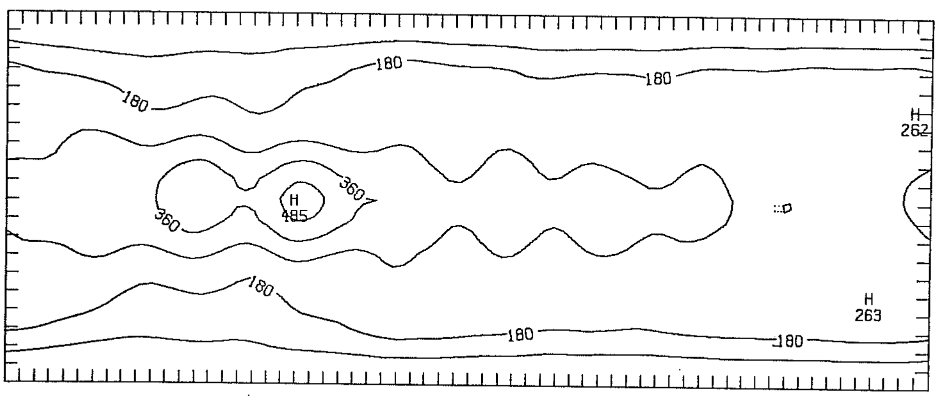

Figure 5 : High-pass component of the variance of streamfunction at mid-level.

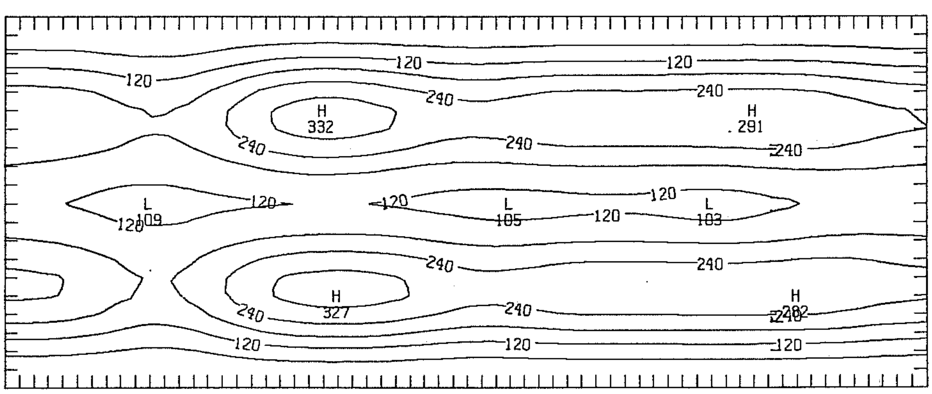

Figure 6 : Low-pass component of the variance of streamfunction at mid-level.

We now apply a high-pass filter to the spatial spectral domain and consider only wavenumbers with $k \geqslant 4$ or $l \geqslant 3$. The high pass variance, Fig. 5, is now entirely concentrated within a storm track located in the center of the channel and extending well beyond the exit of the jet. The associated heat variance and fluxes turn out to be very similar to the total quantities displayed in Fig. 4.

The low-pass variance, for wavenumbers with $k \leqslant 3$ and $l \leqslant 2$, is shown in Fig. 6. It concentrates in two parallel branches centered at 1/4 and 3/4 of channel width. A well marked dipole is observed at the exit of the jet. Heat variance and fluxes are one order of magnitude smaller than the high-pass contribution ; they reduce the baroclinicity in the center of the channel and reinforce it near the boundaries.

The observed splitting of variance is very similar to the result of Shutts (1983). However, his artificial wavemaker is replaced here by a localized area of increased baroclinicity.

Nonlinear equilibration

The above analysis is highly suggestive of the existence of a zonal regime during which the perturbations develop and propagate along a storm track well beyond the end of the jet, and a blocking regime characterized by strong diffluence of the wind at the exit of the jet which blocks the perturbations.

Indeed, sequences of this kind are easily found by visual inspection of a long time integration of the model. The aim of this section is to show that they correspond to two different equilibria of the flow.

The main difficulty is that we cannot just look for simple stationary flows since we expect that transient fluxes contribute in a significant way to the maintenance of large-scale stationary structures. Indeed we only wish to fix the large-scale components of the flow - as defined above in the analysis of low-pass variance - and let the other components evolve freely. The equilibration must be obtained by time averaging the contribution of small-scale activity to the largest scales. In shorthand notations, the problem is formulated as

$$0 = \dot{S} = A(S,S) + B(S,\overline{V}) + \overline{C(V,V)} + L(S) \qquad (3)$$

where S stands for the large-scale components of the flow and V for the small-scale components. A,B and C are nonlinear terms which couple the large-scale components together and with small-scale components. L groups all the linear terms, planetary advection, dissipation and large-scale part of the forcing. The overbar denotes a time average. In order to use minimization procedures, and since S is a vector in phase space with 28 components, we define a cost function as

$$J = \langle \dot{S}, \dot{S} \rangle$$

where <.,.> is a scalar product, actually the energy of the tendency $\dot{S}$.

Starting from a given distribution of large-scale components S_0, we want to minimize J and eventually converge to zero. We use a conjugate-gradient algorithm (Gill et al., 1982) which requires knowledge of the gradient of J with respect to the components of S. It is quite straightforward to obtain by formal differentiation the contribution from the terms which depend only on S in the right hand side of (3). The main difficulties arise with the computation of the B and C terms and their gradients. The method used here is to integrate first the model for a very long time and then to use the archived history records as an interactive data base in the optimization process. $\overline{V}$ and the transients forcing $\overline{C(V,V)}$ are obtained for a given S from a sample of the archived records which satisfy a proximity criterion to S based on the large-scale components only. More precisely, we record the following quantities each five days of a run of 15000 days : the large-scale components S_i, the small-scale components $\hat{V}_i$ and transient flux $\hat{C}_i(V,V)$ averaged over five days where i denotes sampling time. Then for a given $\tilde{S}$, we define

$$\bar{V}(\tilde{S}) = \frac{\sum_i \Phi(||\tilde{S}-S_i||).\hat{V}_i}{\sum_i \Phi(||\tilde{S}-S_i||)}$$

and $$\bar{C}(\tilde{S}) = \frac{\sum_i \Phi(||\tilde{S}-S_i||).\hat{C}_i}{\sum_i \Phi(||\tilde{S}-S_i||)}$$

where $\Phi(d)$ is a smooth proximity function which verifies $\Phi(0)=1$; $\Phi(d)=0$ for $d>d_0$. The radius d_0 is chosen such that about 200 records are selected among 3000.

From this point, and since Φ is differentiable, there are no considerable difficulties in getting the gradient of V and C through calculation of adjoint operators (Le Dimet and Talagrand, 1986).

Zonal and blocking régimes

The procedure sketched above was applied starting from different initial S_0, taken from the integration run. We present here results based on a proximity function Φ which is local in physical space, i.e. we consider only the field located in the first half of the channel in longitude. In addition, only antisymmetric modes are considered since the solution is expected to be antisymmetric. However, the cost function is computed over the whole channel.

Four solutions are obtained which minimize J. Three of them converge exponentially to zero and the fourth one corresponds to a non zero, but very small, minimum. The four solutions exhibit in fact only two different patterns which are shown in Fig. 7 and 8 for two selected solutions. The imposed jet is present in the first third of the channel with about the same profile for both solutions. In the middle third, the two solutions differ drastically; a clear dipole structure appears in Fig. 8 when the solution shown in Fig. 7 remains almost zonal. Fig. 9 shows the variations of the cost function J, as S is interpolated and extrapolated from the two solutions shown in Fig. 7 and 8. 0 stands here for the zonal solution and 1 for the blocked solution. The two solutions are clearly separated and the residual cost is five orders of magnitude smaller than values obtained for interpolated fields.

It is now important to investigate in which respect the small-scale fluxes are different from one of the two regimes to the other. Fig. 10 and 11 show separately the different terms which balance in the right hand side of equation (3). In both cases, the large-scale terms A and L (Figs. 10 a-b, 11 a-b) tend to dissipate the wave structure, i.e. only the jet in the zonal case, the jet and the dipole in the blocked case. The B(S,V) term (Fig. 10 c-d, 11 c-d) acts to damp the upstream part of the baroclinic jet and to extend it downstream. It does not play a significant role in the blocking area. The most interesting contribution is due to the $\overline{C(V,V)}$ term (Fig. 10 e-f, 11 e-f). The first effect is to extend the jet downstream with the strongest tendency in the lower layer, i.e. with damping of the baroclinicity. In the zonal regime, this effect dominates the first half of the channel. Its extension is limited to the first third in the blocking case. In this regime, the mid-channel is occupied by a reverse structure which forces the diffluence of the jet and the generation of a blocking dipole.

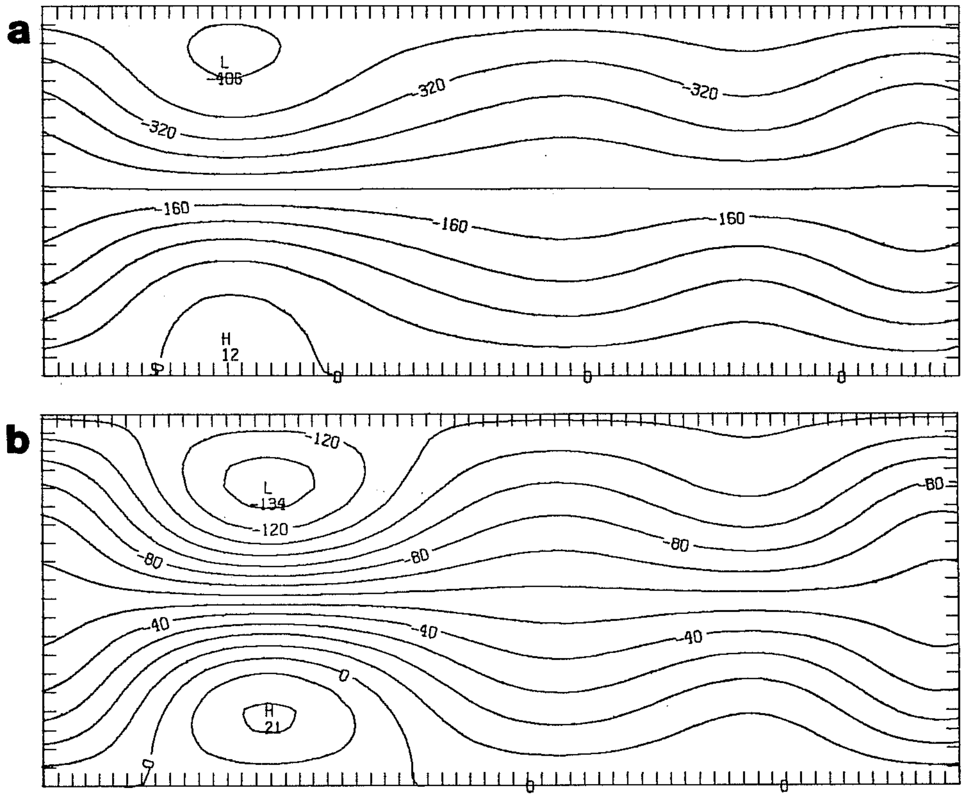

Figure 7 : Streamfunction of a zonal-type equilibrium.
a) upper layer b)lower layer.

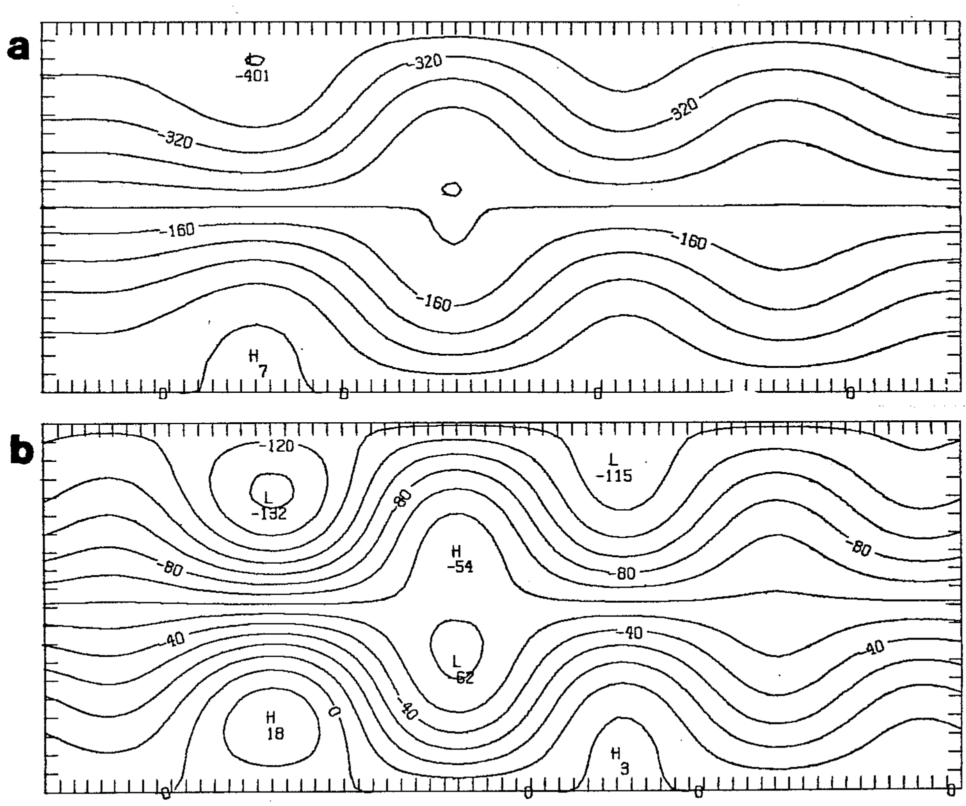

Figure 8 : Same as 7 for a blocking-type equilibrium.

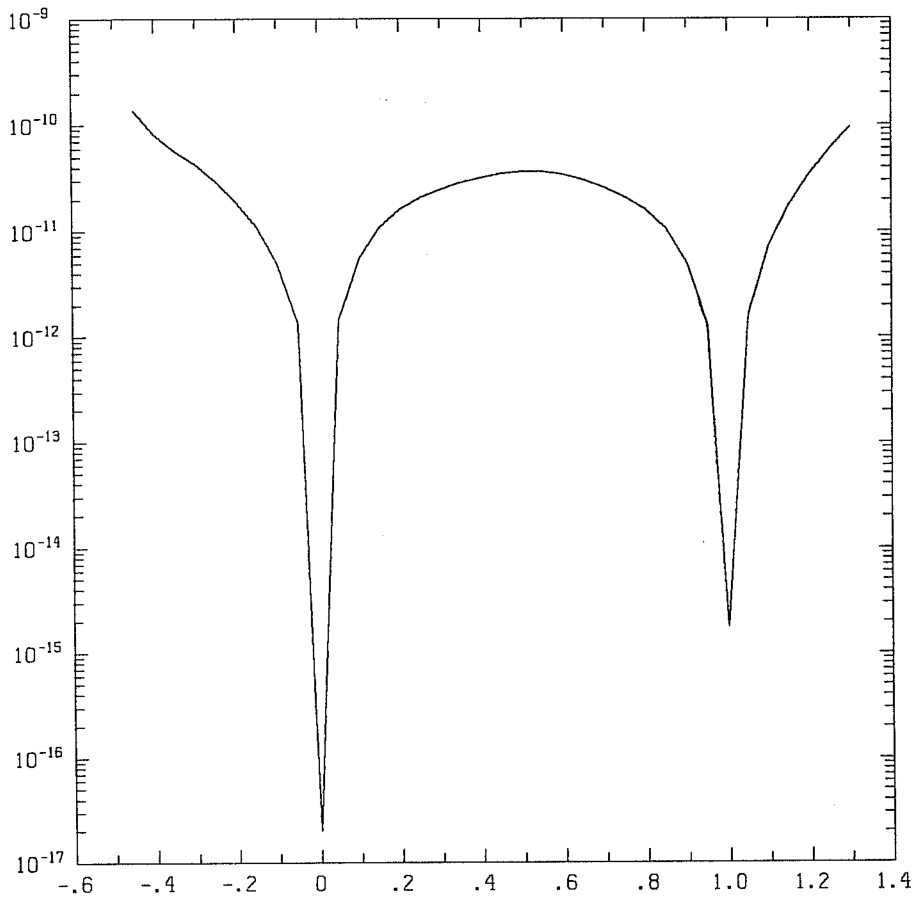

Figure 9 : Variation of the cost function on a segment of phase space which contains the two equilibria shown in Fig. 7 and 8. 0 stands for the zonal solution and 1 for the blocked solution.

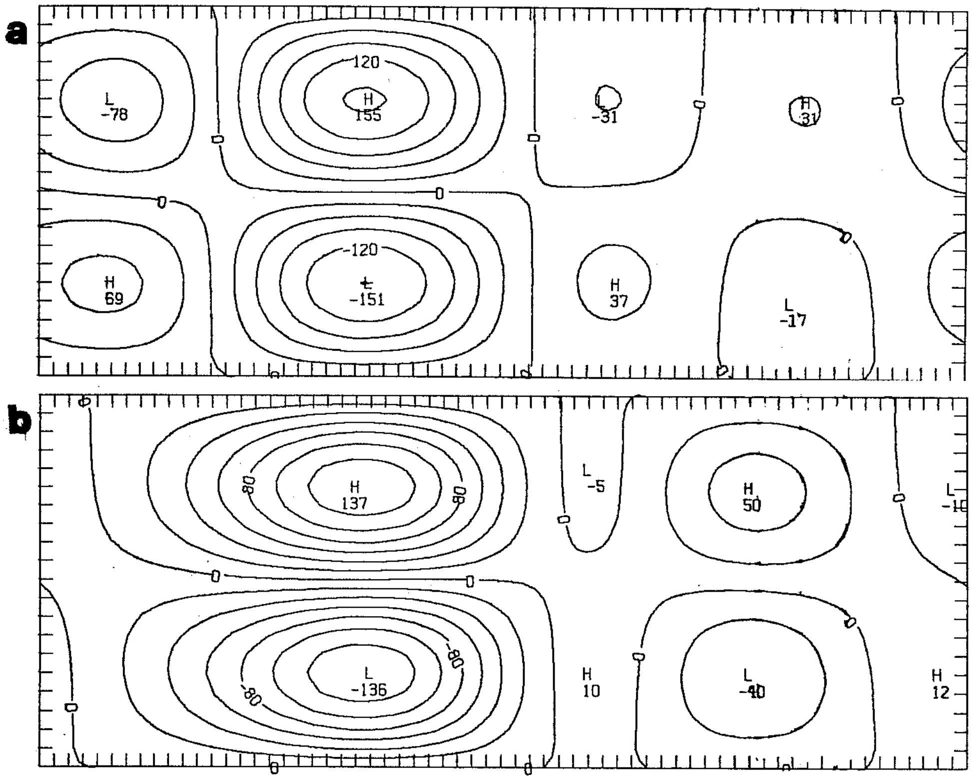

Figure 10 : Contributions to the right hand side of (3) for the zonal regime

- large-scale terms $A(S,S)+L(S)$ a)upper layer b)lower layer
- coupling term $B(S,\bar{V})$ c)upper layer d)lower layer
- forcing by the transients $\overline{C(V,V)}$ e)upper layer f)lower layer

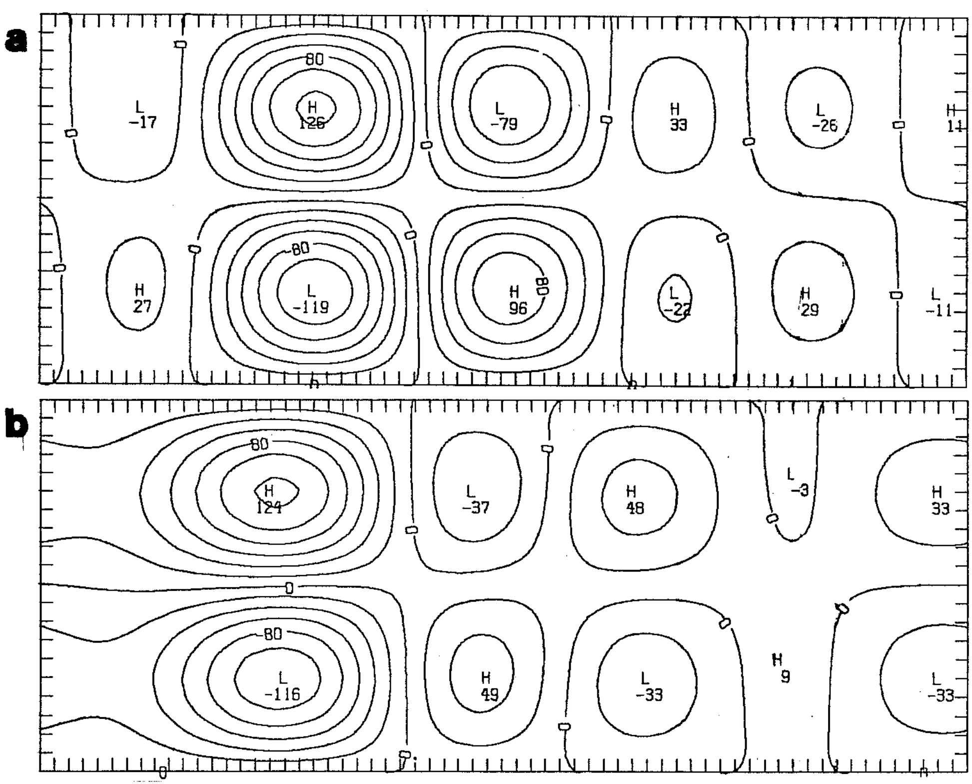

Figure 11 : Same as figure 10 for the blocked regime.

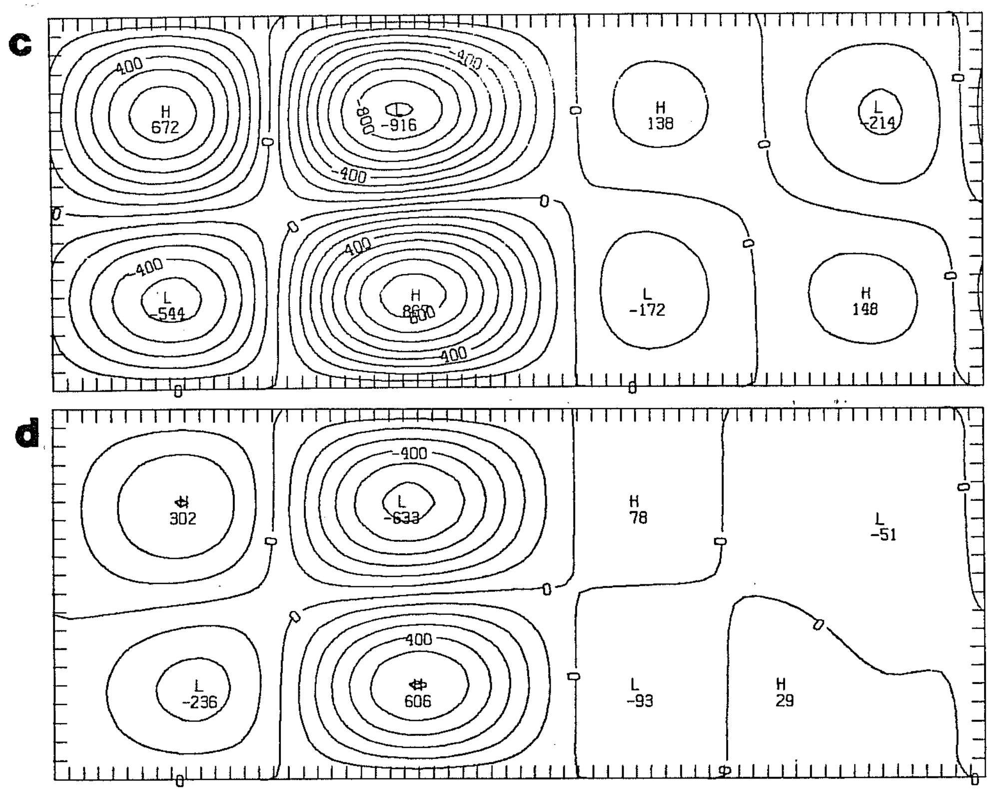

Figure 10 (Continued)

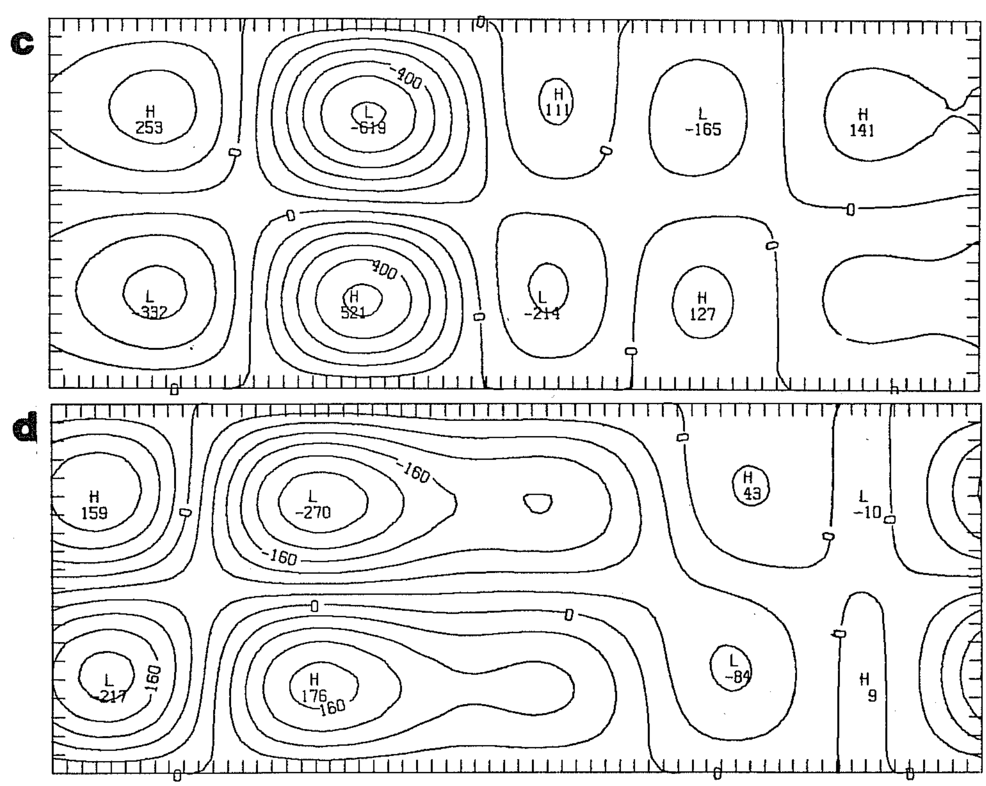

Figure 11 (Continued)

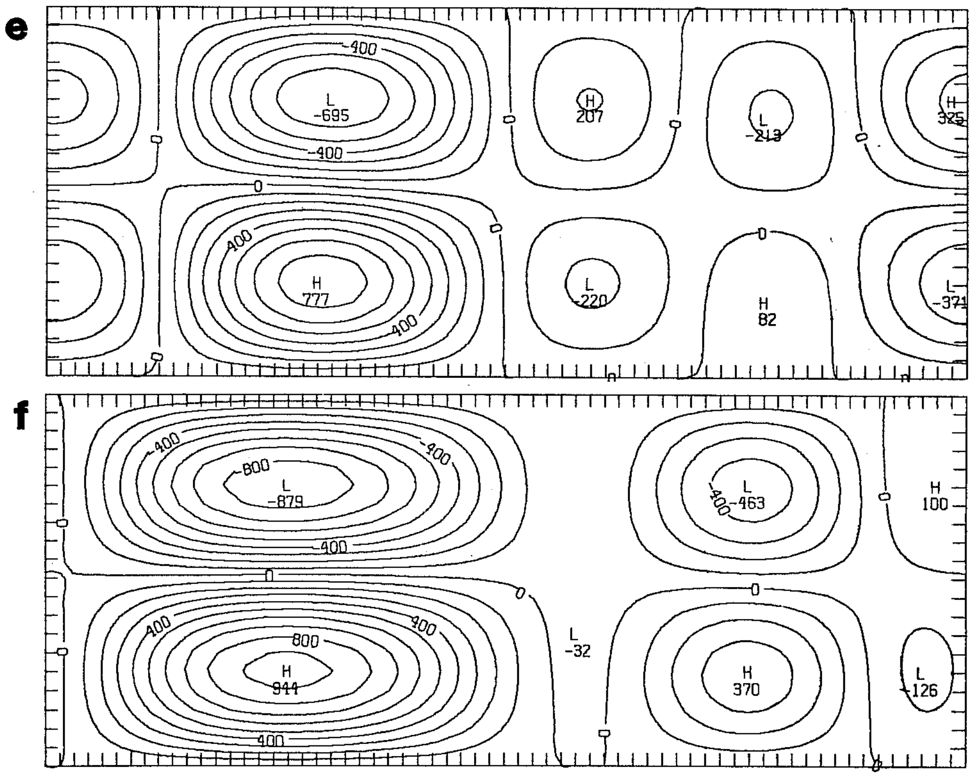

Figure 10 (Continued)

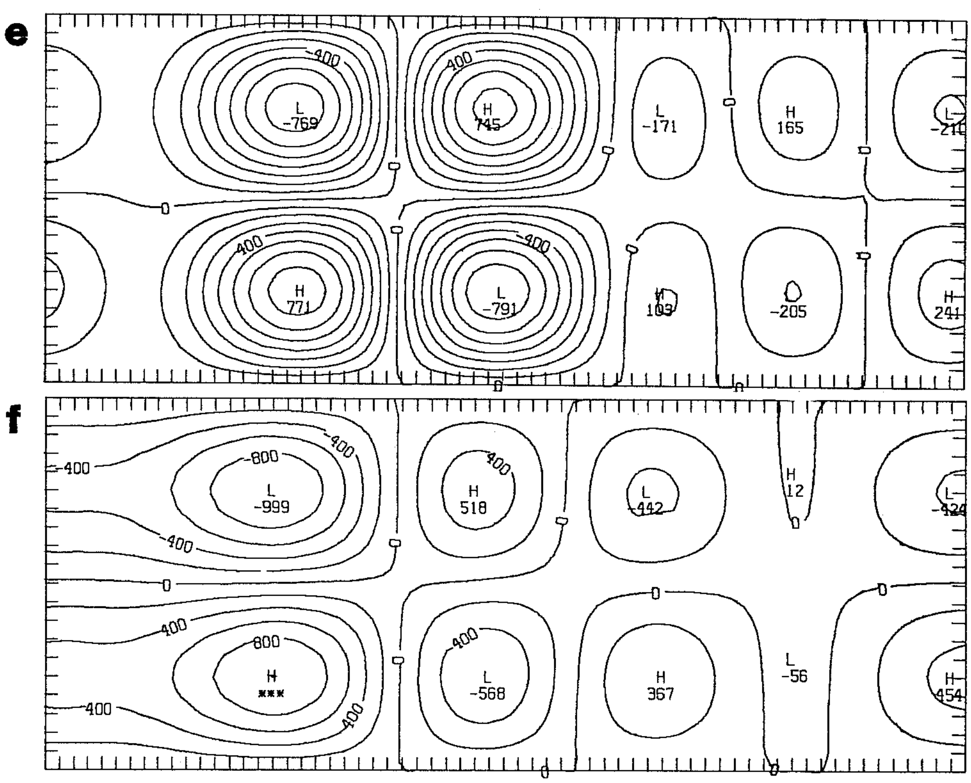

Figure 11 (Continued)

Thus, the small-scale transients do not play a simple diffusive role in our model. They contribute to maintain the barotropic part of the jet and they generate a blocking dipole at the exit of the jet. Although this analysis is based on spatial scale separation and not on time filtering, it is perfectly consistent with the observations of Hoskins et al.(1983) on time-filtered high-pass transients. Moreover, if we add our terms A and B we recover a pattern similar to their low-pass forcing of the mean flow. The novelty here is that we are able to distinguish two different flow regimes, with respectively zonal and blocking patterns, which correspond to two different balances of the right hand side of (3).

Discussion

The existence of multiple flow regimes proceeds from the inhomogeneities of the phase-space of the investigated model. Instead of being an ellipsoid centered on the representative point of the averaged circulation, the 'cloud' of accessible states possesses a complex structure with several concentrations of the measure, the centers of which appear as equilibria in our method.

It was shown in Legras and Ghil (1985), in the framework of a barotropic model, that these inhomogeneities induce naturally a flow dependency of the predictability properties. Basically, one can distinguish the predictability of flow regimes from the usual point-wise predictability, the former being linked with the existence of multiple regimes. The simplest hypothesis is to expect that the exit from a given regime is governed by a Markovian process and thus that the probability distribution of residence time near the equilibria decrease exponentially with the duration.* This behavior is indeed observed, both in the analysis of atmospheric data (Dole and Gordon, 1983) and in the simple model investigated by Legras and Ghil(1985). A similar analysis is currently undertaken for the baroclinic model presented in this study.

There are indications from the present study and previous work (Egger and Schilling, 1983; Reinhold and Pierrehumbert, 1982) that transitions between regimes are largely caused by synoptic-scale activity but we must also take in account the possibility that large-scale instabilities (Frederiksen, 1982) trigger the transition mechanism. An intricate question, which has still to be clarified, is how the destabilisation effect of small scales is combined with the positive feedback which plays a major role in the maintenance of large-scale flow. A second important question is how the variations of external conditions, such as sea surface anomalies, modify the equilibria and their transition properties . For large variations typical of the seasonal cycle, the existence of multiple equilibria is likely to induce abrupt breaks in weather regimes through hysteresis effects instead of smooth variations with the external conditions. A well known example is the onset of the Indian monsoon regime which takes only a few days to change completely the wind circulation over the whole Indian Ocean and a part of Asia (Krishnamurti et al, 1981). The interannual variations of external conditions are not expected to overcome the internal variability in mid-latitude, except in some extreme cases (e.g. when a giant cloud of dust produced by a major volcanic explosion such as the Krakatau). The extend to which the modulation of internal variability can be predicted is a challenge for future work.

---

* This can be demonstrated if one is able to derive a potential function for the system (Schuss, 1981). See Dole and Gordon (1983) for an attempt to determine such a function from atmospheric data.

The more familiar concept of pointwise or deterministic predictability arises from the irreversible growth of small errors. In phase space, two trajectories starting close to each other tend to diverge with an exponential averaged rate. Legras and Ghil (1985) found that this rate depends largely on the weather regime.

Furthermore, equilibria are not the sole possible regularity of phase space. Reproducible sequences of patterns may appear which correspond to pieces of attractor in which trajectories are transversaly confined, although the timing may vary from one case to the other. An example of such an event is shown in Legras and Ghil (1984). This might account for the frequent observation of events of this type in the atmosphere, although true cycles cannot generally be detected.

The method used in this study can be easily generalized to a more realistic model, like a simplified general circulation model. It provides an efficient way to tackle the problem of multiple regimes within the large scales. More generally, it can be applied to the study of the parameterization of small-scale activity when scales are separated in both wavenumber and frequency domains. A major difficulty lies in the choice of the cut in wavenumber domain and of the proximity function. The latter must clearly be determined by physical considerations and the former may be suggested by the analysis of stationary and propagative variance (Hayashi, 1982). Fourier modes are certainly not the best choice to project the solution. Attractive alternates - which bring however an additional complexity to the method - are eigenmodes of the linearized problem or local modes derived by weakly non-linear analysis (Malguzzi and Manalotte-Rizzoli, 1984). It must be noted that, when looking for equilibria, the method always converges to a minimum of the cost function. Consistency checks have to be performed to verify that this minimum is much smaller than the averaged value of the cost function and that persistence sequences are associated with the obtained pattern.

Acknowledgments

We thank Pierre Bernardet, Philippe Courtier, Michael Ghil, Dennis Hartmann and Olivier Talagrand for useful discussions. Claude Lemaréchal (INRIA) provided us with the code for conjugate gradient algorithm (M1GC2). The manuscript was typed by Mlle Marie-Christine Cally.

The computer resources used in this study were allocated by the Scientific Council of the Centre de Calcul Vectoriel pour la Recherche. Figures were plotted by the NCAR Graphics Software.

REFERENCES

BAUR, F., 1951, Extended range weather forecasting, Compendium of Meteorology, Amer. Met. Soc., 814-833.

BENZI, R., HANSEN, A.R. and A. SUTERA, 1984, On stochastic perturbation of simple blocking models, Quart. J. R. Met. Soc., 110, 393-410.

CHARNEY, J.G. and J.G. DEVORE, 1979, Multiple flow equilibria in the atmosphere and blocking, J. Atmos. Sci., 36, 1205-1216.

CHARNEY, J.G., SHUKLA, J. and K.C. MO, 1981, Comparison of a barotropic blocking theory with observation, J. Atmos. Sci., 38, 762-779.

DOLE, R.M. and N.D. GORDON, 1983, Persistent anomalies of the extratropical Northern Hemisphere winter time circulation : Geographical distribution and regional persistence character, Mon. Wea. Rev., 111, 1567-1586.

EGGER, J., 1981, Stochastically driven large-scale circulation with multiple equilibria, J. Atmos. Sci., 38, 2606-2618.

EGGER, J. and H. D. SCHILLING, 1983, On the theory of the long-term variability of the atmosphere, J. Atmos. Sci., 40, 1073-1085.

FREDERIKSEN, J. S., 1982, A unified three-dimensional theory of the onset of blocking and cyclogenesis, J. Atmos. Sci., 39, 969-982.

GILL, P. E., MURRAY, W. and M.H. WRIGHT, 1982, Practical optimization, Academic Press, London, 401 p.

HANSEN, A., 1985, Observational characteristics of atmospheric planetary waves with bimodal amplitude distribution, in Global scale anomalous circulation and blocking, eds R. Benzi, A. Wiin Nielsen and B. Saltzman, Adv. in Geophys., 29, Academic Press, New York, in press.

HAYASHI, Y., 1982, Space-time spectral analysis and its applications to atmospheric waves, J. Meteor. Soc. Jap., 60, 156-171.

HOSKINS, B.J., I.N. JAMES and G.H. WHITE, 1983, The shape, propagation and mean-flow interaction of large scale weather systems, J. Atmos. Sci., 40, 1595-1612.

ILLARI, L. and J.C. MARSHALL, 1983, On the interpretation of maps of eddy fluxes during blocking episodes, J. Atmos. Sci., 40, 2232-2242.

ITOH, H., 1985, The formation of quasi-stationary waves from the viewpoint of bifurcation theory, J. Atmos. Sci., 42, 917-932.

KALLEN, E., 1984, Bifurcation mechanisms and atmospheric blocking, in Problems and Prospects in Long and Medium Range Weather Forecasting, eds D. M. Burridge and E. Kallen, Springer-Verlag, 229-263.

KALLEN, E., 1985, An hysteresis-like effect in orographically forced models, Tellus, 37a, 249-257.

KRISHNAMURTI, T. N., ARDANAY, P., RAMANATHAN, Y. and R. PASCH, 1981, On the onset vortex of the summer monsoon, Mon. Wea. Rev., 109, 344-363.

LE DIMET, F. X. AND O. TALAGRAND, 1986, Variational algorithms for analysis and assimilation of meteorological observations : theoretical aspects, Tellus, 38A, 97-110.

LEGRAS, B. and M. GHIL, 1984, Blocking and variations of atmospheric predictability, Predictability of Fluid Motions, G. Holloway and B. J. West, Eds, American Institute of Physics, 87-105.

LEGRAS, B. and M. GHIL, 1985, Persistent anomalies, blocking and variations in atmospheric predictability, J. Atmos. Sci., 42, 433-471.

MALGUZZI, P. and P. MANALOTTE-RIZZOLI, 1984, Nonlinear stationary Rossby waves on nonuniform zonal winds and atmospheric blocking. Part I : The analytical theory, J. Atmos. Sci., 41,2620-2628.

REINHOLD, B.B. and R.T. PIERREHUMBERT, 1982, Dynamics of weather regimes : Quasi-stationary waves and blocking, Mon. Wea. Rev., 110, 1105-115.

SCHUSS, Z., 1981, Singular perturbation methods in stochastic differential equations of mathematical physics, SIAM Rev., 22,2,119-155.

SHUTTS, G. J., 1983, The propagation of eddies in diffluent jetstreams : eddy vorticity forcing of blocking flow fields, Quart. J. R. Met. Soc., 109, 737-761.

SIMMONS, A. J. and B.J. HOSKINS, 1978, The life cycles of some nonlinear baroclinic waves, J. Atmos. Sci., 35, 414-432.

TUNG, K. K. and A. J. ROSENTHAL,1985, Theories of multiple equilibria. A critical reexamination. Part I : barotropic models, J. Atmos. Sci., 42, 2804-2818.